DEVELOPMENT OF A DISCHARGE ESTIMATION METHOD FOR FROZEN RIVERS

By

Yasuhiro Yoshikawa

Civil Engineering Research Institute for Cold Region, Sapporo, Hokkaido, Japan

Yasuharu Watanabe

Kitami Institute of Technology, Kitami, Hokkaido, Japan

Hiroshi Hayakawa

Kitami Institute of Technology, Kitami, Hokkaido, Japan

and

Yasuyuki Hirai

Civil Engineering Research Institute for Cold Region, Sapporo, Hokkaido, Japan

SYNOPSIS

Flow discharge during the period when a river is frozen over is the important data for a long term full-year plan of water resources plan. Detailed field observations were carried out at three sites in the Teshio River in Hokkaido, Japan. The techniques for presuming energy gradient, open water area, hydraulic radius and flow velocity coefficient were shown in the analysis of the observation. The relation between flow velocity coefficient, hydraulic radius and energy gradient was clarified in a frozen river. A method for estimating flow discharge of a frozen river using C, river width B_w and discharge area A_o was developed. The accuracy of this estimating flow discharge was approximately 92% of 36 data with a margin of error of 20% plus or minus.

INTRODUCTION

The annual lowest discharge of rivers is often recorded during the freezing season, and serves as an important source of data when developing year-round water resource plans. Since the freezing season in Hokkaido lasts from late December to early April (approximately 100 days), accurate estimation of river discharge during this period is also important for river management in the future, when winter discharge is anticipated to increase as a result of climate change.

In the open water season, continuous discharge is estimated from the water level measured continually using the water level-discharge curve (H-Q curve), which indicates the relationship between the water level H and the discharge

Q. Kamata (1) pointed out that the relationship between the water level and discharge in the freezing season differs from that in the open water season, since the water levels are affected by the bed height, effective depth and draft depth of river ice, and that it is more practical to find the relationship between the effective depth and the discharge.

Under the current method for estimating discharge when open waters are frozen over based on the above, the equivalent water level *H*' is found by substituting the observed discharge during this season into the *H-Q* curve of the open water season, and the difference ΔH (= $H - H'$) between the observed water level *H* and the equivalent water level *H*' are estimated. Then, the continuous equivalent water level *H*' is calculated by subtracting ΔH from the continually measured water level *H*, and the continuous discharge in the freezing season is estimated by substituting this equivalent level *H*' into the *H-Q* curve of the open water season. This method incorporates the influences of the coefficient of roughness for the river ice bottom, the river ice area and the energy gradient into the increase in water level ΔH. The coefficient of roughness for the river ice bottom and the river ice area were found to vary over time in past studies (2) (3), and the energy gradient affects discharge in the freezing season (4). Accordingly, ΔH is thought to be non-unique, as it is affected by freezing conditions and hydraulic phenomena.

To address this problem, Hirayama (5) (6) (7) presented a method for estimating ΔH by introducing a parameter *K*. His method uses the roughness coefficient and the energy gradients in the open water and freezing seasons to estimate ΔH, and obtains the equivalent water level in the open water season from that in the freezing season *H* using the *K*. While the application of this method is limited to sections where frazil does not accumulate, it can evaluate appropriately the influences of the coefficient of roughness for the river ice bottom, the river ice area and the energy gradient, and the estimated discharge corresponds well with observed values (83% of all 58 data sets were within a margin of error of ±20%). It has also been shown that *K* is closely correlated to ice sheet thickness. However, this method is not applied to actual sites at present, since sections where frazil accumulates remain outside the scope of application of the technique, and sufficient understanding is lacking in relation to large fluctuations in *K*, which have been pointed out in areas with large variations in the coefficient of roughness for the river ice bottom.

In any case, the current method estimates discharge in the freezing season from the *H-Q* curve of the open water season by correcting the water level in the freezing season *H* to the equivalent water level in the open water season *H'* on the assumption that the *H-Q* curve is not effective in the freezing season. This means that the accuracy of the estimated discharge is affected by the accuracy of the *H-Q* curve for the open water season.

In this study, a detailed field observation was conducted to enable the development of a discharge estimation method for the freezing season using observed data. A technique was presented to estimate the energy gradient, discharge area, hydraulic radius and flow velocity coefficient in the freezing season by simply adding the water level measurement at a single site to the current observation items, and a new method of estimating discharge in the freezing season without depending on the *H-Q* curve of the open water season was developed by using only data for the current observation items.

FIELD OBSERVATION

A detailed field observation was conducted from January to March 2008 at three sites – Site A (Maruyama Observatory, KP30.00), Site B (Ponpira Observatory, KP58.93) and Site C (Onnenai Observatory, KP111.70) – on the Teshio River (channel length: 256 km; catchment area: 5,590 km^3) in northern Hokkaido. KP (an abbreviation of kilo post) values represent the distance from the estuary in kilometers. In this study, ice in the frozen river was roughly divided into hard ice sheets and soft frazil located on the water surface and under ice sheets. The river water surface was completely covered with ice at all three sites during the observational period. Frazil accumulation was more pervasive at Site C than at Site A and Site B. Fig. 1 shows the locations and lateral profiles of Sites A, B and C.

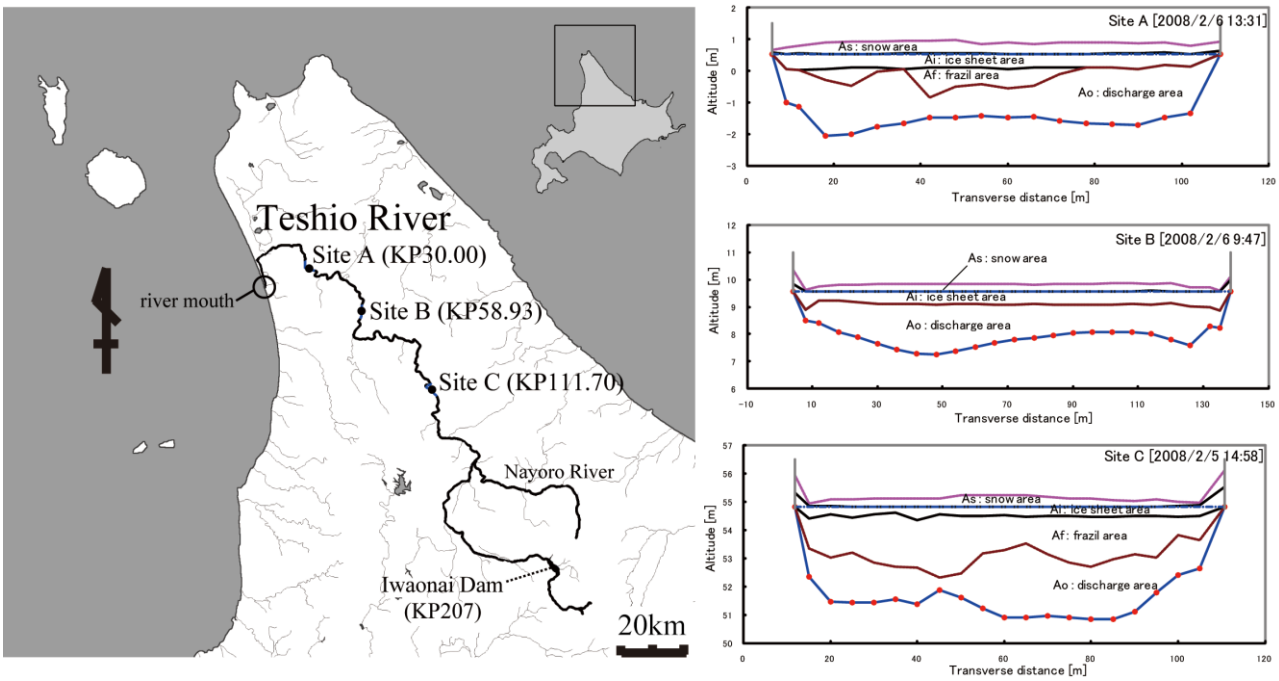

Figure 1 Observation Sites and transverse surveying in the Teshio River

The water level and discharge were observed at each section. The water level was measured by using an absolute pressure water level gauge with a data logger (Mc-1100, Koshin Denki Kogyo Co., Ltd., measurement accuracy: ±1 cm), and the flow velocity was measured using an electromagnetic velocity meter for rivers (AEM1-D, Alec Electronics Co., Ltd., measurement accuracy: ±0.005 m/s or ±2% of the measured value). Measurements were taken every 10 minutes during the observation period, and precise discharge observations were conducted 10 times at Site A and Site B and 20 times at Site C by setting the velocity measurement intervals to 10 cm in the depth direction to obtain accurate values. Flow velocity measurements were conducted at points marked in red on the lateral profiles in Fig. 1, which were set at intervals of approximately 5 m. More detailed observations were conducted at Site C, since we found from past observation results to have greater frazil fluctuations. For the measurement of flowing water, ice sheet and frazil areas, water levels on the staff gauge were read based on the assumption that the water level in the transverse direction of the observation section was uniform without vertical fluctuation during the observational period. The distances from the water surface to the riverbed, frazil and ice sheets were measured at the four corners of the observation holes using straight poles and L-shaped poles, and the average results were taken as the measured values. Frazil measurement requires a high level of skill. At Site A and Site B, the water levels were measured every 10 minutes, and low-discharge observations were conducted 10 times at a point 250 m upstream of each observation site. At Site C, the water level was measured every 10 minutes at a point 400 m upstream of the observation site. The upstream points were selected in line with site conditions.

FACTORS AFFECTING OBSERVED DISCHARGE IN THE FREEZING SEASON

Factors affecting the observed discharge were examined based on the observed values, with a focus placed on the discharge area, hydraulic radius, flow velocity coefficient and energy gradient. The discharge area is the area in which water flows.

Temporal changes in freezing conditions and hydraulic phenomena

Fig. 2 shows the observed discharge Q [m^3/s], discharge area A_o [m^2], ice sheet area A_i [m^2], frazil area A_f [m^2] and Manning's coefficient of roughness n [$s/m^{1/3}$] obtained by field observations. As Manning's coefficient of roughness, the value of the compound roughness for the riverbed and ice bottom was determined from the observed values such as

$$n = \frac{A_o R^{\frac{2}{3}} I_e^{\frac{1}{2}}}{Q} \tag{1}$$

The hydraulic radius R [m] was found from the discharge area and the wetted perimeter, and the energy gradient I_e [non-dimensional] was found by substituting the sectional average flow velocity u_m [m/s] and the water level H [m] into the momentum equation.

$$I_e = -\frac{d}{dx}\left[\alpha \frac{u_m^2}{2g} + H\right] \tag{2}$$

Here, g [m/s^2] is 9.8, and the energy coefficient α [non-dimensional] is 1.1. Since the upstream sectional average flow velocity u_m was not measured at Site C, the water surface gradient I_w was assumed to be the energy gradient I_e. It can be seen from Fig. 2 that temporal variations in the frazil area A_f depends on the site, while the ice sheet area A_i increased over time at all sites. While Manning's coefficient of roughness varied between 0.012 and 0.038 at Site A, it ranged from 0.026 to 0.083 and decreased over time at Ponpira. The value at Site C was 0.126 to 0.042 and also decreased over time, but the fluctuation was sharper compared with that seen at Ponpira. The results of the detailed field observation revealed that freezing conditions and hydraulic phenomena depends on the sites.

Correlation between observed discharge and various values

Table 1 shows the correlation between the discharge Q observed at each site and four factors (discharge area A_o, hydraulic radius R, flow velocity coefficient ϕ and energy gradient I_e. In this study, the flow velocity coefficient ϕ [non-dimensional] expressed by Eq. 3 was used to clarify the hydraulic significance of Manning's coefficient of roughness. In Eq. 3, u_* [m/s] represents the friction velocity ($=\sqrt{gRI_e}$).

$$\phi = \frac{u_m}{u_*} = \frac{R^{\frac{1}{6}}}{n\sqrt{g}} \tag{3}$$

Table 1 shows that the correlation of the observed discharge Q with A_o and R was high at Site A but low at Site B and Site C, that the correlation with ϕ was relatively similar at all sites, and that the correlation with I_e was higher at Site A and Site C than at Site B. While the relationship of the observed discharge Q with the effective depth h_w and energy gradient I_e have been mentioned out in past studies (1) (4), it was presumed from the detailed field observations results in this study that such relationships are not applicable to all sites despite a certain correlation, and that these factors cannot be determined as unambiguously as in the open water season. Since the discharge in the freezing season is thought to be subject to the combined influences of freezing conditions and hydraulic phenomena, it was necessary to consider them in a balanced manner. The effective depth h_w and the hydraulic radius R are approximately related by $h_w \simeq 2R$.

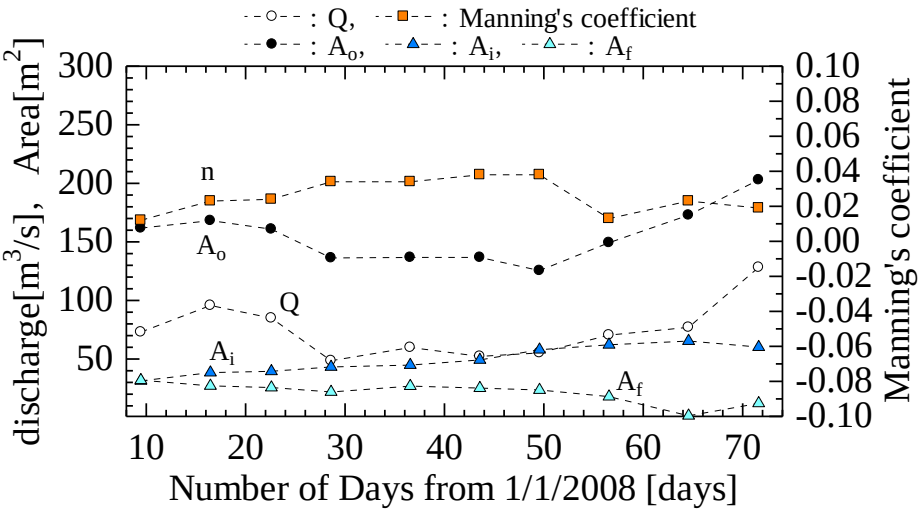

1) Site A

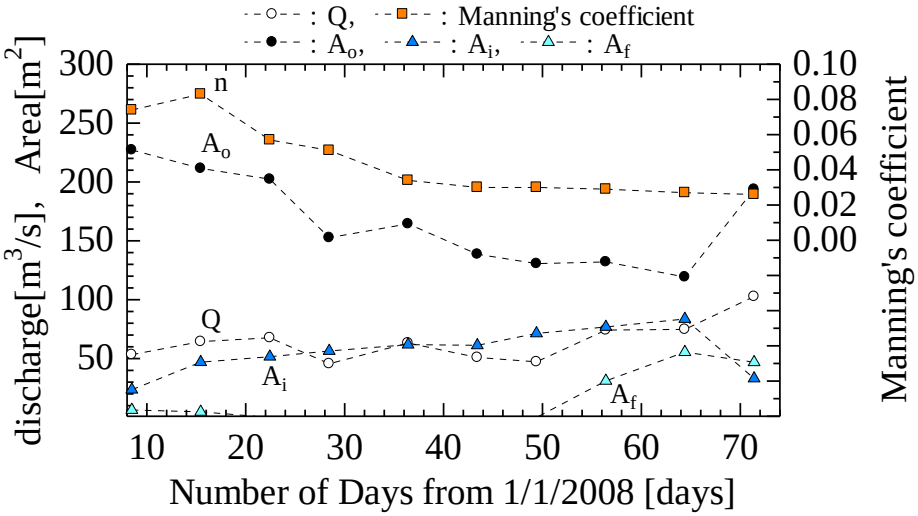

2) Site B

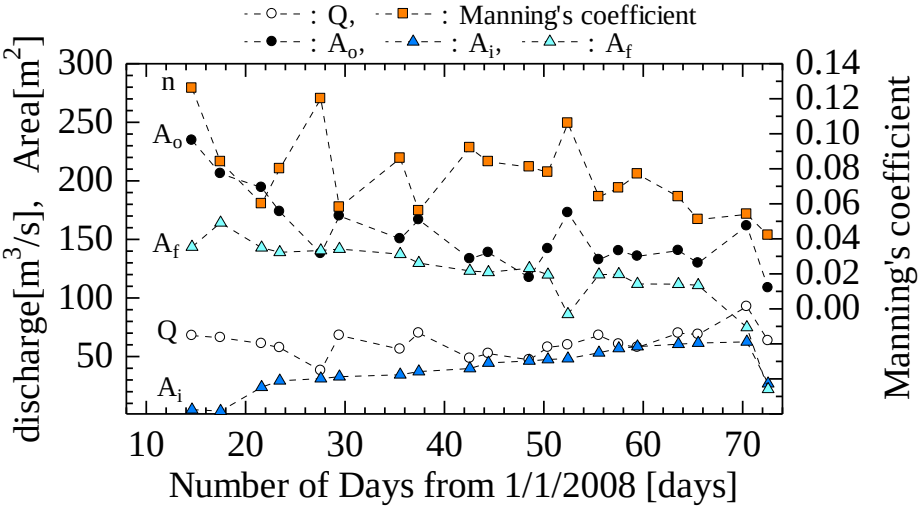

3) Site C

Figure 2 Field observed results

Table 1 Coefficient of correlation(r) between observed discharge and four factors

a coefficient of correlation r	A_o	R	ϕ	I_e
Site A	0.940	0.934	0.401	0.463
Site B	0.154	0.132	0.493	0.151
Site C	0.302	0.318	0.611	0.436

METHOD OF ESTIMATING DISCHARGE IN THE FREEZING SEASON

A basic equation was adopted to estimate discharge in the freezing season was formulated in this study as shown below.

$$Q = A_o \, \phi \sqrt{gRI_e} \tag{4}$$

As the field observation results showed that factors affecting the observed discharge in the freezing season cannot be determined, methods of estimating the values of A_o, R, I_e and ϕ were individually considered. Then, a method for estimating the discharge in the freezing season was developed based on these study results.

Estimation of energy gradient I_e

Assuming that the flow is uniform during the observation of discharge in the freezing season, the relationship between the energy gradient I_e and the surface gradient I_w can be expressed by

$$I_e \simeq I_w \tag{5}$$

Fig. 3 illustrates the relationship between the water surface gradient I_w and the energy gradient I_e. The values correspond well with each other, indicating that the water surface gradient I_w measured in the freezing season can be used to approximate the energy gradient I_e.

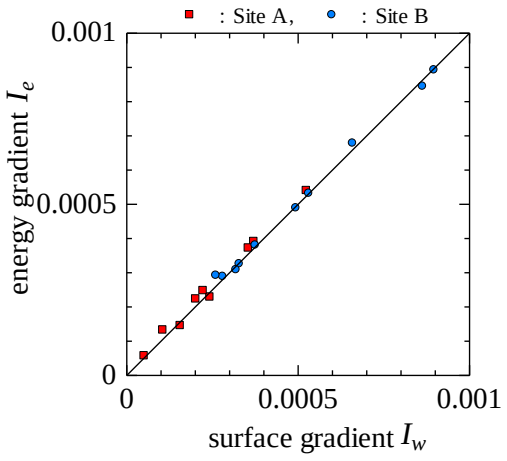

Figure 3 Energy gradient and Surface gradient

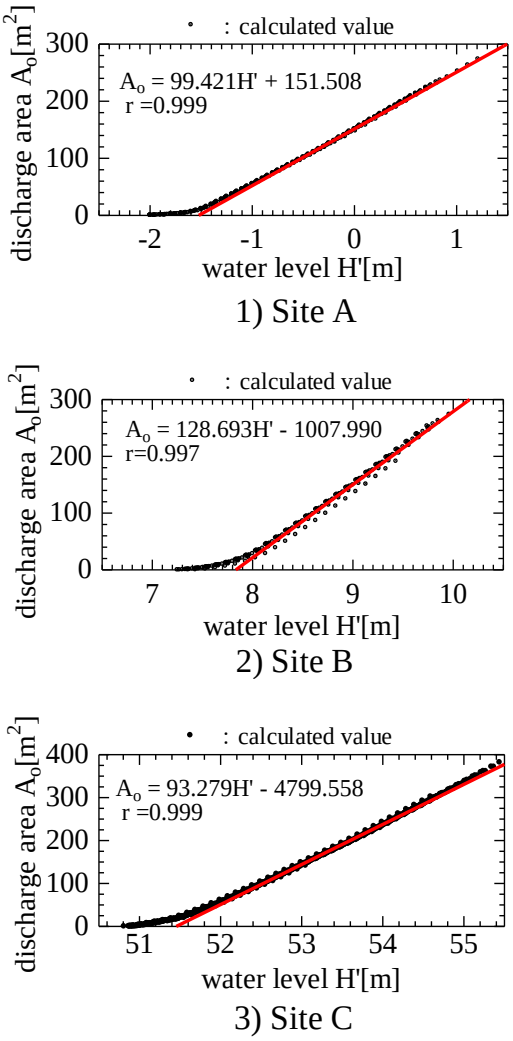

Figure 4 Relationship between the water level H' and the discharge area A_o

Estimation of discharge area A_o and hydraulic radius R

The discharge area A_o was estimated by finding the relationship between the water level H' and the discharge area A_o as shown in Fig. 4 in advance using transverse survey data from the open water season. Furthermore, the water level H' was estimated by using Eq. 6 from the water level H and the draft d in the freezing season. The water level H' in the freezing season is the altitude for the river ice bottom, such that

$$H' = H - d \tag{6}$$

$$d = \frac{\rho_s A_s + \rho_i A_i + \rho_f A_f}{\rho_w B_w} \tag{7}$$

Here, B_w [m] denotes the river width, ρ [kg/m^3] is the density. The density values for water, snow, ice and frazil were ρ_w = 1000.00, ρ_s = 100.00, ρ_i = 917.40 and ρ_f = 950.38, respectively. In this study, ρ_f is the density which is mixed frazil and water.

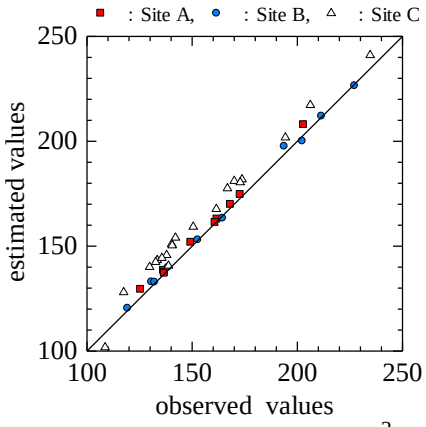

1) discharge area A_o [m^2]

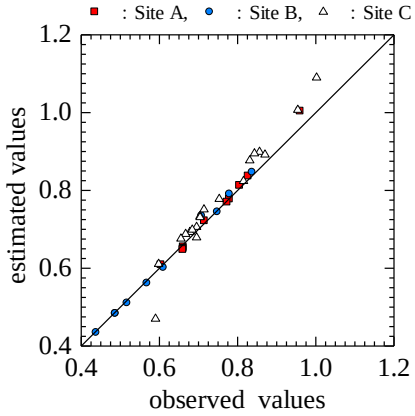

2) hydraulic radius R [m]

Figure 5 Observed and Estimated values of A_o and R

When deriving the draft d in Eq. 7, the river ice and bank conditions are free (1) and not fixed since the draft of river ice fluctuates vertically with changes in the water level. By dividing A_i into the ice sheet area above A_{iu} [m^2] and below the water level A_{id} [m^2], and assuming that river ice is subject to buoyancy, the weight of the floating body in air $\rho_s g A_s + \rho_i g\,(A_{iu} + A_{id}) + \rho_f\, gA_f$ is equal to the level of buoyancy $\rho_w g\,(A_{id} + A_f)$. Assuming that $(A_{id} + A_f) = B_w d$, the draft d can then be expressed by Eq. 7. If the river ice area is observed regularly, there is a simple method of ascertaining the ice area by means of linear supplement. As for the meaning of linear supplement, the period without data acquired the value, when data and data were connected in a straight line.

The hydraulic radius R can be expressed by using the values for the wetted perimeter of the river ice S_i [m] and the riverbed S_b [m], such that

$$R = \frac{A_o}{S_i + S_b} \simeq \frac{A_o}{2B_w} = \frac{h_w}{2} \tag{8}$$

Assuming that $B_w \gg h_w$ and $S_i \simeq S_b \simeq B_w$, the hydraulic radius R can be expressed by the effective depth h_w. The effective depth h_w can be estimated with the average bed height Z [m], such that

$$h_w = H - d - Z \tag{9}$$

The value of Z was found to be -1.441 m at Site A, 7.898 m at Site B and 51.604 m at Site C from the transverse survey results.

Fig. 5 illustrates the observed and estimated values of A_o and R. It can be seen from the figure that the observed values are reproduced accurately by the estimates.

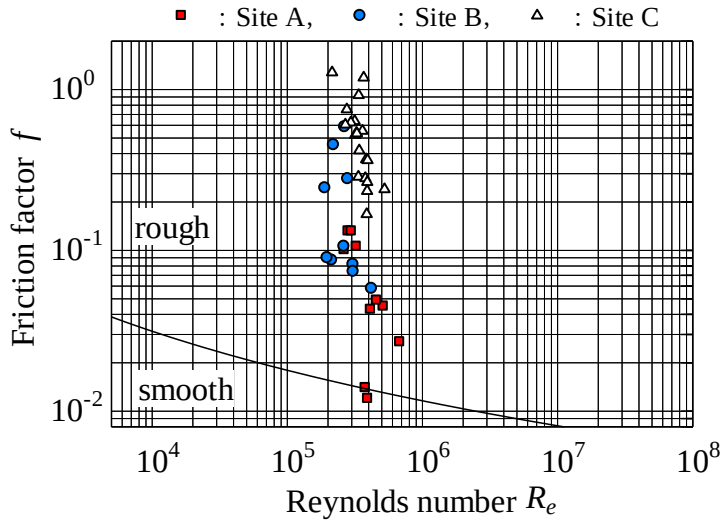

Figure 6 Friction factors for Frozen Rivers

Estimation of velocity coefficient ϕ

Since basic understanding of the flow velocity coefficient ϕ in the freezing season is not sufficient at present, focus was placed on the equivalent roughness k_s, which is a function of ϕ, and its variation factors were examined to present an equation for the estimation of ϕ in this study.

Since pressure in a frozen river is released through cracks of the river ice, the flow in the freezing season is not a pipe flow in a hydrological sense; it is presumed to be the same as a pipe flow if one considers only the phenomenon in which flowing water is affected by energy loss caused by friction resistance at the riverbed and ice at the bottom, which are the surfaces of contact with the flowing water. In this study, the flow path in the freezing season was thought to have the characteristics of pipe flow. Energy loss in a pipe flow can be expressed by the equation of Darcy-Weisbach (Eq. 10), which can be rearranged with the flow velocity coefficient ϕ into Eq. 11. Here, f [non-dimensional] is the friction factor, D is the pipe diameter, and their relationship is $D = 4R$.

$$I_e = \frac{f}{D}\frac{u_m^2}{2g} \tag{10}$$

$$\phi = \sqrt{8/f} \tag{11}$$

To determine whether the wall of the pipe flow in the freezing season is smooth or rough, f was found by substituting ϕ (estimated from the observed value using Eq. 3) into Eq. 11, and the relationship between f and R_e (= Ru_m/v) was plotted on the Moody (9) diagram. Fig. 6 shows the results. As the dynamic viscosity coefficient v [m^2/s], the value at 0°C (1.785×10^{-6}) was given. It can be seen from Fig. 6 that 2 out of 40 data sets were in the smooth pipe range, while the remaining 38 were in the completely rough range. The wall of the frozen river as a pipe flow was thus determined to be rough, as 95% of the observed values out of the 40 data sets in total were in the completely rough range, despite the fact that two were in the smooth range. The two data sets in the smooth pipe range were observed at Site A. These data were obtained in the first (January 10) and eighth (February 26) of the ten observations. Since the energy gradient I_e were 0.000041 and 0.000057, it was deduced that f was underestimated in these instances. However, as some other days of observation were close to a new or full moon, the blockage of flowing water by river ice accumulated upstream was also thought to be attributed to this phenomenon. No further clarification of the matter is available at present.

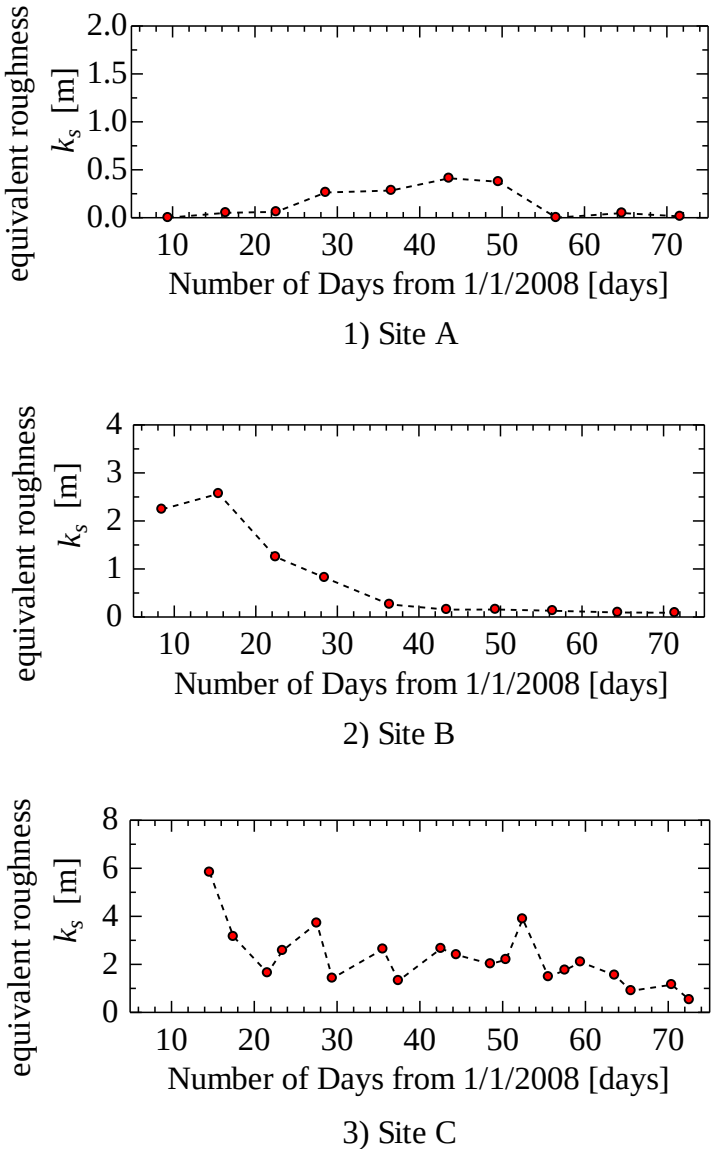

Figure 7 Temporal changes in k_s

The equivalent roughness k_s (10) was estimated by using Eq. 12, the relationship between f and k_s for rough walls, to clarify temporal changes in k_s.

$$\frac{1}{\sqrt{f}} = 2.0 log_{10} \frac{7.40D}{2k_s} \tag{12}$$

Fig. 7 shows the temporal changes in k_s [m]. While the value varied between 0.0004 and 0.4111 at Site A, it ranged from 0.0874 and 2.5670 and decreased over time at Site B. At Site C, it ranged from 0.5252 to 5.8330 and decreased over time with fluctuations. Compared with Sites B and C, k_s of Site A increased until the 40th day. Since Site A is located downstream from the other two sites, river ice flowing from upstream was more likely to accumulate under the ice sheets. It was therefore deduced that the shape of the river ice at the bottom changed with the passage of time, and that accumulated river ice increased k_s, which indicates the roughness of the river ice at the bottom at Site A.

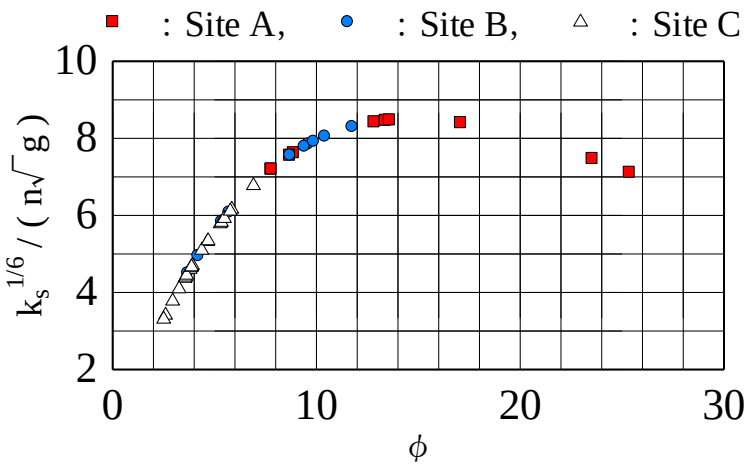

Figure 8 Manning-Strickler equation ϕ vs $k_s^{1/6} / (n\sqrt{g})$

Since it can be deduced from Fig. 2 that these fluctuations are similar to those of Manning's coefficient of roughness, the Manning-Strickler equation (Eq. 13) was adopted to determine the relationship between ϕ and $k_s^{1/6} / (n\sqrt{g})$ as shown in Fig. 8.

$$\phi = \frac{k_s^{\frac{1}{6}}}{n\sqrt{g}} \left(\frac{R}{k_s}\right)^{\frac{1}{6}} \tag{13}$$

Fig. 8 shows that ϕ ranges between 2 and 25. Since the velocity coefficient ϕ of pipe and open channel flows are usually around 8 to 25, $k_s^{1/6} / (n\sqrt{g})$ is approximated to be 7.66 for practical reasons. However, the small value of ϕ in the field survey results of this study indicates that $k_s^{1/6} / (n\sqrt{g})$ cannot be assumed to be a constant in the freezing season.

Variations in materials of river-bed and river-ice, the shapes of the river-bed and river-ice were thought to be variation factors behind the decrease in k_s over time as shown in Fig. 7. Assuming that riverbed variations are negligibly small in the freezing season (the period in which the annual lowest discharge is often recorded), fluctuations in k_s are caused by variations in constituent materials and the shape of the river ice bottom. Air temperature, water temperature and flow velocity are thought to be the factors affecting the constituent materials and the shape of the river ice bottom. In particular, flowing water is thought to cause melting and smoothing of the river ice bottom and results in a reduction of the equivalent roughness k_s.

This study was conducted with the assumptions below. Variations in the materials of river ice were not taken into account, and focus was placed only on variations in the shape of the river ice bottom. Variations in this shape were evaluated by assuming that the ice thickness near flowing water affecting the bottom shape was h_{id} [m] and identifying temporal changes (dh_{id} / dt) in this value. Since the air temperature often fell below zero during the observational period, it cannot be seen as the main cause of the river ice melting. Accordingly, melting as the main cause of variations in the shape of the river ice bottom was represented by the heat flux from the flowing water to the river ice bottom, and variations in the bottom shape resulting from this flux were expressed by Eq. 14. Fig. 9 shows images of the time progress in the shape of the river ice. Photo. 1 shows the actual river ice bottom at Site C. It can be seen from the figure that the bottom is not flat.

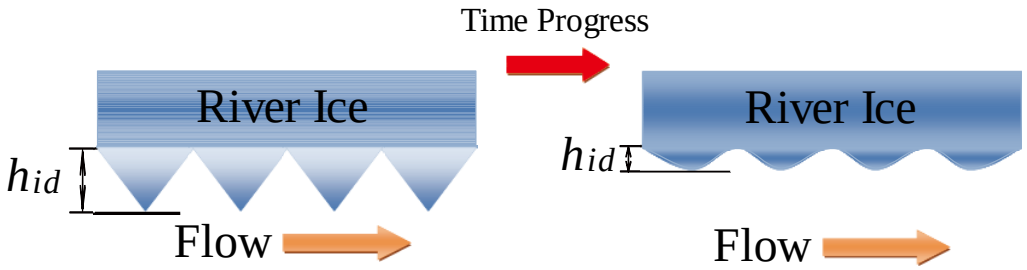

Figure 9 Image figure of time progress in the shape of the river ice

Photograph 1 shows the actual the bottom of river ice at Site C.
It can be seen from the figure that the bottom is not flat.

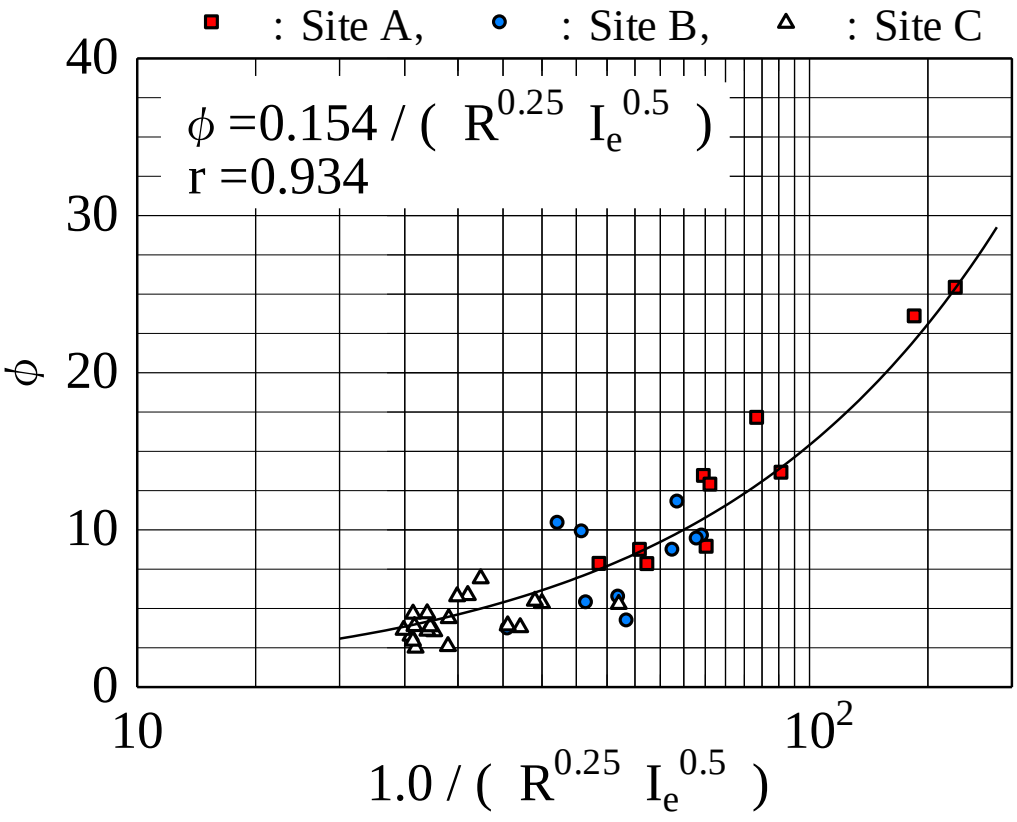

Figure 10 1.0 / ($R^{0.25}$ $I_e^{0.5}$) vs ϕ

$$\rho_i L_i \frac{dh_{id}}{dt} = -\phi_w \tag{14}$$

$$\phi_w = C_{wi} \frac{u_m^{0.8}}{h_w^{0.2}} (T_w - T_{id}) \tag{15}$$

Here, L_i [J/kg] is the latent heat of ice and h_{id} [m] is the river ice thickness near the flowing water, and the heat flux from the flowing water to the river ice bottom ϕ_w [W/m^2] can be expressed by Eq. 15 (11). C_{wi} is 1622 W・S$^{0.8}$・°C^{-1}・m$^{-2.6}$, T_w [°C] is the water temperature, and T_{id} [°C] is the temperature at the river ice bottom (0°C).

By substituting Eq. 15 into Eq. 14 and defining C_o [m$^{1/4}$] using Eq. 17 and arranging it with the flow velocity coefficient ϕ, Eq. 16 can be derived. Fig. 10 shows the relationship between 1.0 / ($R^{0.25}$ $I_e^{0.5}$) and ϕ in Eq. 16. While there are errors caused by setting dh_{id}/dt and T_w in Fig. 10, the correlation coefficient for all data was 0.934, indicating a high correlation.

$$\phi = \frac{C_o}{R^{0.25} I_e^{0.5}} \tag{16}$$

$$C_o = \left(-\frac{dh_{id}}{dt} \frac{\rho_i L_i 2^{\frac{1}{5}}}{C_{wi} T_w g^{\frac{2}{5}}} \right)^{\frac{5}{4}} \tag{17}$$

Estimation equation for discharge in the freezing season

To estimate discharge in the freezing season, Eq. 18 is formulated by substituting the estimation equations for the energy gradient Eq. 5, hydraulic radius Eq. 8 and flow velocity coefficient ϕ Eq. 16 into the basic equation for discharge calculation Eq. 4 and defining C [m$^{3/4}$/s] using Eq. 19. C denotes the degree of decrease in roughness caused by melting and smoothing of the river ice bottom by flowing water. In this estimation equation, riverbed variations are not taken into consideration, so riverbed roughness is thought to be constant and its influence is assumed to be incorporated in C:

$$Q = C B_w^{-\frac{1}{4}} A_o^{\frac{5}{4}} \tag{18}$$

$$C = \left(-\frac{dh_{id}}{dt} \frac{\rho_i L_i}{C_{wi} T_w} \right)^{\frac{5}{4}} \tag{19}$$

$$C = C_o \left(2^{-\frac{1}{4}} g^{\frac{1}{2}} \right) = \phi u_* h_w^{-\frac{1}{4}} \tag{20}$$

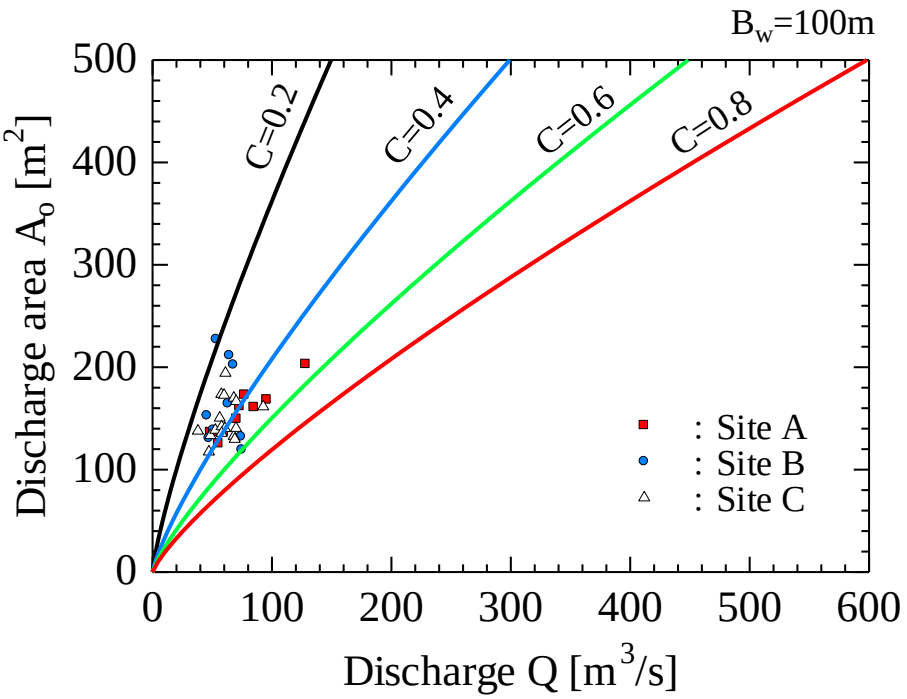

Figure 11 Discharge Q and Discharge area A_o in response to variations in the C value

The discharge Q and discharge area A_o in response to variations in C increasing of this estimation equation are shown in Fig. 11. The figure illustrates that the discharge area A_o decreases with increasing amounts of river ice, and that the discharge Q decreases with C caused by the rough river ice bottom in the estimation equation.

On the assumption that $C = \tilde{C}\check{C}$, for example, where ˜ denotes the normalized constant and ˇ represents a dimensionless quantity, Eq. 21 can be derived by non-dimensionalizing Eq. 18. Eq. 22 can be obtained through normalization with

$$(\tilde{C}\tilde{A}_o^{\frac{5}{4}})/(\tilde{Q}\tilde{B}_w^{\frac{1}{4}}) = 1$$

$$\check{Q} = \left[\frac{\tilde{C}\tilde{A}_o^{\frac{5}{4}}}{\tilde{Q}\tilde{B}_w^{\frac{1}{4}}}\right] \times \check{C}\,\check{B}_w^{-\frac{1}{4}}\,\check{A}_o^{\frac{5}{4}} \tag{21}$$

$$\tilde{C} = \tilde{u_m}\,\tilde{h_w}^{-\frac{1}{4}} \tag{22}$$

The normalized constant for each value was set to satisfy Eq. 22 by assuming $\tilde{Q} = 1$ as shown in Table 2. From Eq. 21 and Table 2, Eq. 18 is expressed by

$$Q = \check{C}\left(\frac{B_w}{\tilde{B}_w}\right)^{-\frac{1}{4}}\left(\frac{A_o}{\tilde{A}_o}\right)^{\frac{5}{4}} \tag{23}$$

As $\check{C}$ is the function of the flow velocity coefficient ϕ and the equivalent roughness k_s, it changes over time. Fig. 12 shows the temporal changes in $\check{C}$ obtained by substituting the observed values of this study into Eq. 18 to find C and non-dimensionalizing it with $\tilde{C}$. Fig. 12 shows that the degree of roughness decreases because $\check{C}$ increases in relative terms over time even though temporal changes in $\check{C}$ vary as observed at the station.

Table 2 Normalized constants used in the discharge estimation equation for the freezing season

$\tilde{Q}$	$\tilde{A}_o$	$\tilde{B}_w$	$\tilde{C}$	$\tilde{u_m}$	$\tilde{h_w}$
1	10	10	0.1	0.1	1

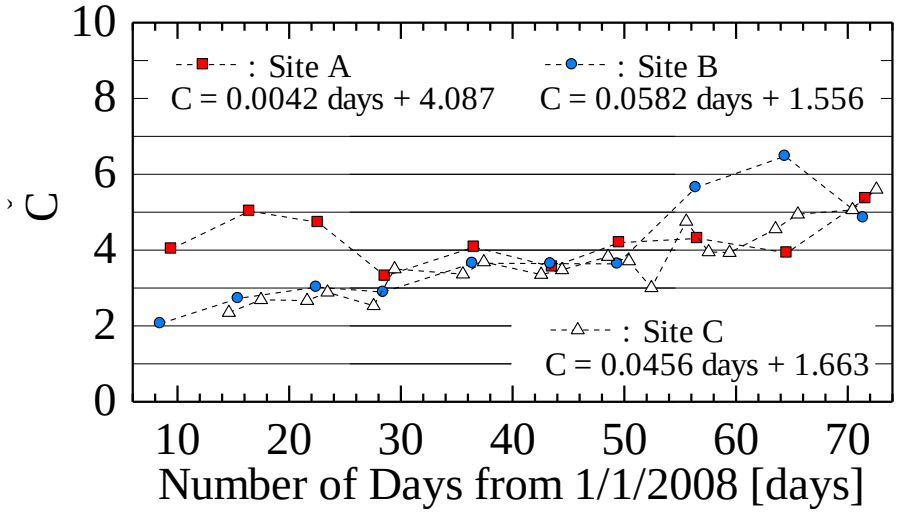

Figure 12 Temporal changes in $\check{C}$ (non-dimensional) and the estimation equation (observation data of this study)

ACCURACY COMPARISON FOR DISCHARGE ESTIMATION METHODS IN THE FREEZING SEASON

Based solely on existing observation data, discharge was estimated by using three methods with *ΔH*, *K* or *C* (the new method in this study), and discharge observed in this study were assumed to be true values for comparing the accuracy of discharge estimated by each method with the actual observed values to allowing the application of a discharge estimation technique.

It was determined that the input data necessary for estimating discharge should basically include discharge, snow-cover areas, ice sheet areas, frazil areas, river width of water surface and water level as obtained from discharge observed three times a month, and that continuous data concerning the water level should be the hourly values available in the Hydrological and Water Quality Database provided by the Ministry of Land, Infrastructure and Transport.

Discharge estimation procedures for each method

The procedures for estimating discharge using each method are explained below.

a) Method using *ΔH*

1. Derive the *H*-*Q* curve for the open-water season.
2. Substitute the observed discharge *Q* in the freezing season into the *H*-*Q* curve to determine the equivalent water level *H'*.
3. Find *ΔH* (= *H* - *H'*) – the difference between the observed water level *H* and the equivalent water level *H'* during the freezing season. Find *ΔH* for days when no observation was conducted using a linear supplement for the data observed on the preceding and following days.
4. Subtract *ΔH* from the continuous water level *H* in the freezing season and substitute it into the *H*-*Q* curve to estimate the discharge *Q* for the freezing season.

b) Method using the K

The method of using K as outlined by Hirayama (5) (6) (7) is explained here. Applying the Manning equation to the freezing season (indicated by the subscript ***w***) and the open-water season (indicated by the subscript ***s***) gives

$$Q_w = \frac{A_w}{n_0} R_w^{2/3} I_w^{1/2} \tag{24}$$

$$Q_s = \frac{A_s}{n_1} R_s^{2/3} I_s^{1/2} \tag{25}$$

When defining K with Eq. 27, assuming that the values for n_0, n_1, I_w and I_s are constant and the discharges in both seasons are equivalent ($Q_w = Q_s$) in the cross section gives

$$A_s R_s^{2/3} = \frac{1}{K} A_w R_w^{2/3} \tag{26}$$

$$K = \frac{n_0}{n_1} \sqrt{\frac{I_s}{I_w}} \tag{27}$$

If the value on the right of Eq. 26 is continuously given, the resulting value on the left can be used to determine the equivalent water level H'. The discharge can be estimated by substituting the obtained equivalent water level H' into the H-Q curve for the open-water season. Since neither the method of continuously obtaining the value on the right of Eq. 26 nor that of obtaining the equivalent water level from the value on the left is specified in the original publications on the subject (5) (6) (7), we used our own method in this study. The procedure for estimating the discharge is explained in detail below.

1. Derive the H-Q curve for the open-water season, the H-A equation for the open-water season and the H-$A_sR_s^{2/3}$ equation for the open-water season.
2. Obtain $A_wR_w^{2/3}$ using regular observation data from the freezing season. Find the hydraulic radius from Eq. 8.
3. Substitute the observed discharge Q into the H-Q curve and find the equivalent water level H'. Then substitute the equivalent water level H' into the H - $A_sR_s^{2/3}$ equation to find $A_sR_s^{2/3}$.
4. Find K from Eq. 26, the draft d from Eq. 7 and the river width B_w from the observation data. Determine K, d and B_w for days when no observation was conducted using a linear supplement for the data observed on the preceding and following days.
5. Find A_w through substitution of the value obtained by subtracting the draft d from the continuous water level H in the freezing season into the H-A equation. Find the hydraulic radius by substituting A_w and B_w into Eq. 8. Use the obtained values to determine $A_wR_w^{2/3}$.
6. Substitute $A_wR_w^{2/3}$ and K into Eq. 26 and find $A_sR_s^{2/3}$.
7. Substitute $A_sR_s^{2/3}$ into the H - $A_sR_s^{2/3}$ equation to find the equivalent water level H'. Then substitute the equivalent water level H' into the H-Q curve to estimate the discharge Q for the freezing season.

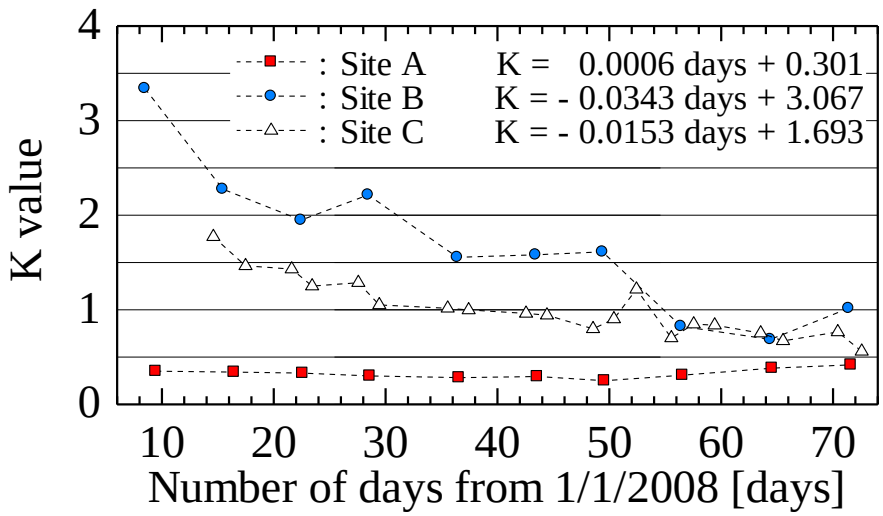

Figure 13 Temporal changes in K and the estimation equation (observation data of this study)

Using the observation data in this study, K was obtained in accordance with the procedure outlined above. Temporal changes in K are shown in Fig. 13, which indicate that temporal changes in K for Site A are smaller than those for the other sites, and that K for sites B and C decreases over time.

Defining K_w by Eq. 28 for the freezing season and K_s from Eq. 29 for the open-water season, K can be expressed as $K = K_s / K_w$. The larger the values of K_s and K_w are, the more easily the water flows.

$$K_w = \frac{\sqrt{I_w}}{n_0} \tag{28}$$

$$K_s = \frac{\sqrt{I_s}}{n_1} \tag{29}$$

K_w was found by substituting the observed data of this study into Eq. 28. Fig. 14 shows K_s, which was back calculated from K and K_w. It can be seen from the figure that K at Site A is small because K_w is larger than K_s and that temporal changes in K are slight due to the small variations in K_w and K_s. In addition, as the degree of river ice roughness is less than that of the riverbed, the compound roughness is smaller than the roughness of the riverbed alone, which results in a larger value of K_w. We found that K is large at sites B and C because K_w in the early stage of the freezing season is smaller than K_s, and that K decreases over time because variations in K_w are larger than those of K_s and K_w increases with time. Assuming that $I_w = I_s$ and n_1 is constant, we inferred that the differences in temporal changes in K from one site to another stem from temporal changes in the compound roughness n as shown in Fig. 2.

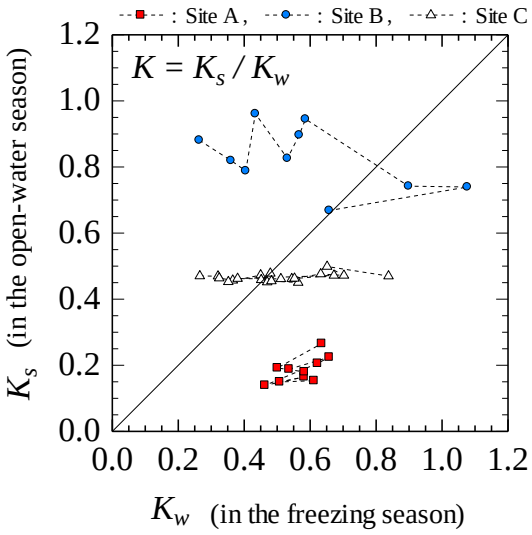

Figure 14 Relationship between K_s (in the open-water season) and K_w (in the freeze-up season)

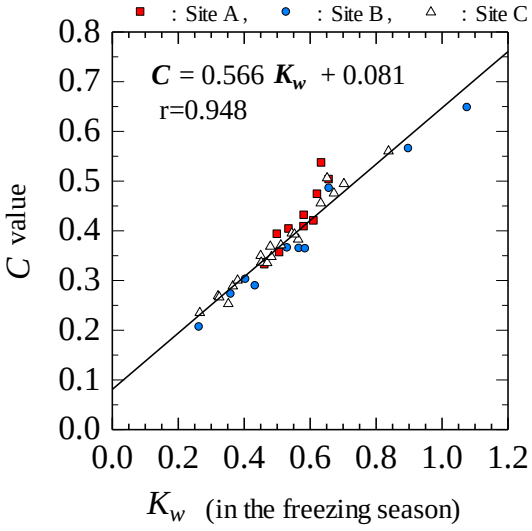

Figure 15 Relationship between C and K_w (in the freezing season)

c) Method using C (new method)

1. Derive a *H-A* equation for the open-water season.
2. Use observed data from the freezing season to find the draft d from Eq. 7 and C from Eq. 18. Obtain the river width B_w from the observed data. Find d, C and B_w for days when no observation was conducted using a linear supplement for the data observed on the preceding and following days.
3. Substitute the value obtained by subtracting the draft d from the continuous water level H in the freezing season into the *H-A* equation to find A_0. Then substitute C, B_w and A_0 into Eq. 18 to estimate the discharge Q for the freezing season.

Using the observed data in this study, C was obtained in the manner described above. The relationship between C and K_w in Eq. 28 is shown in Fig. 15. The observation data suggest that C can be estimated if K_w is known, since there is a close correlation between C and K_w as indicated in the figure.

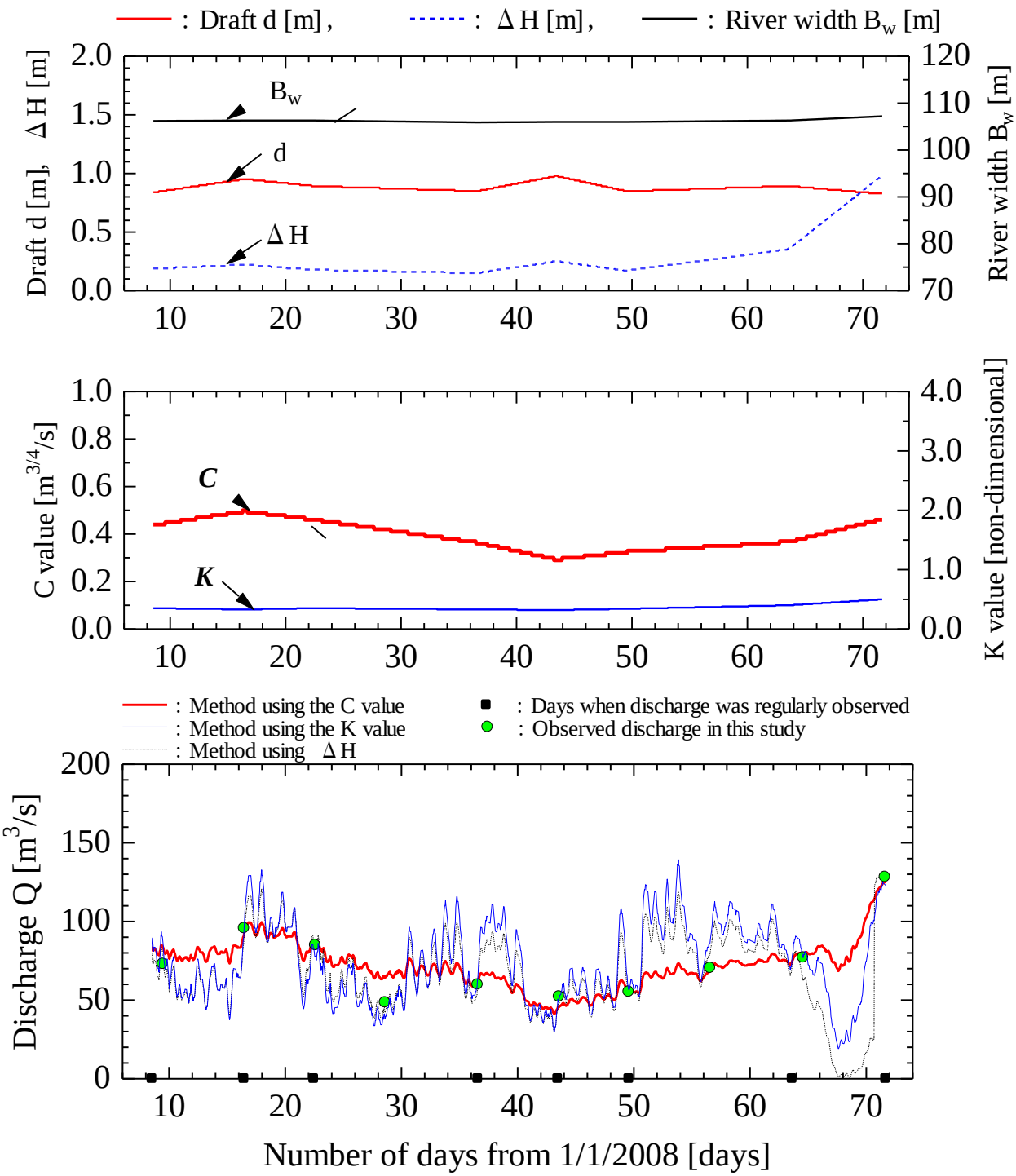

Figure 16 Estimated discharge using the new method vs. the conventional methods and observed discharge (Site A at KP 30.00)

Estimated and observed discharge

Discharge estimated based on existing regular observation data at each site, discharge observed in this study and various data used to estimate discharge are shown in Figs. 16, 17 and 18. The days when observations were conducted are indicated by black squares. These figures reveal that temporal changes in B_w during the observation period are small, and that those in d, ΔH, C and K vary by site. We found that the discharge estimates made using the three methods provide a favorable qualitative reproduction of temporal changes in the observed discharge. Daily fluctuations in discharge were influenced by the volume of water flowing from the Iwaonai Dam located upstream. Fig. 19 illustrates temporal changes in the volume of water discharged by this dam.

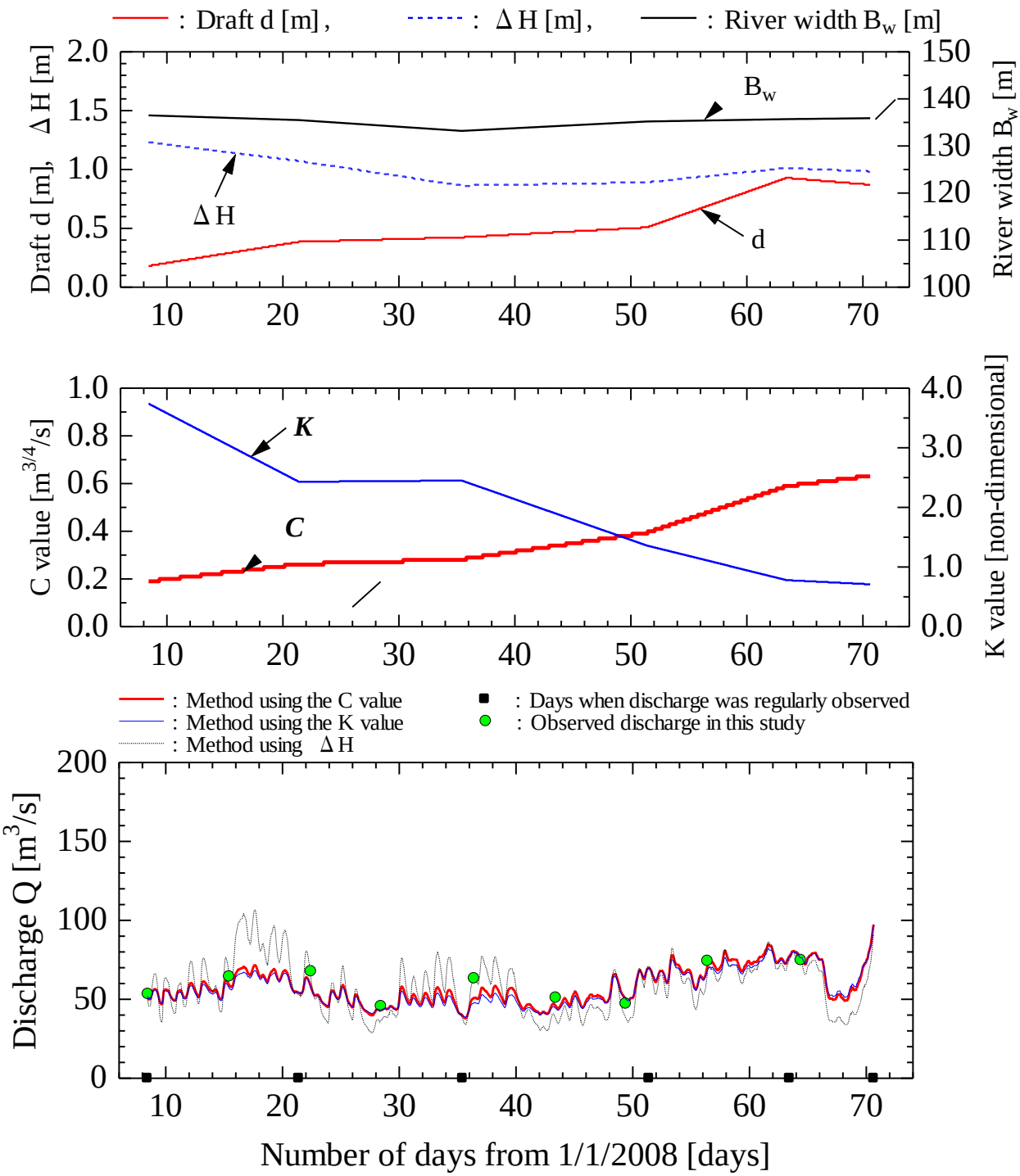

Figure 17 Estimated discharge using the new method vs. the conventional methods and observed discharge (Site B at KP 58.93)

With the method using *ΔH*, discharge is estimated by the water level and *ΔH*. Accordingly it is thought that variations in discharge estimated by the method using *ΔH* are larger than those of the other methods because changes in water level directly reflect changes in discharge. In the method using *K*, fluctuations in *K* become smaller if the fluctuations in bed and river ice roughness are small. Since water-level fluctuations are directly reflected in flow rates when fluctuation in *K* is small, estimated flow rates become sensitive to water-level fluctuations. However, in the method using *C*, fluctuations in *K* can be expressed even if such fluctuations are small. Because of this, there is a considerable difference in estimated flow rates, and the rate estimated by the method using *C* was more accurate at Site A with small fluctuations in *K*, as shown in Fig. 16. Since fluctuations in *K* were significant at Sites B and C as shown in Figs. 17 and 18, the estimation accuracy was similar between the two methods.

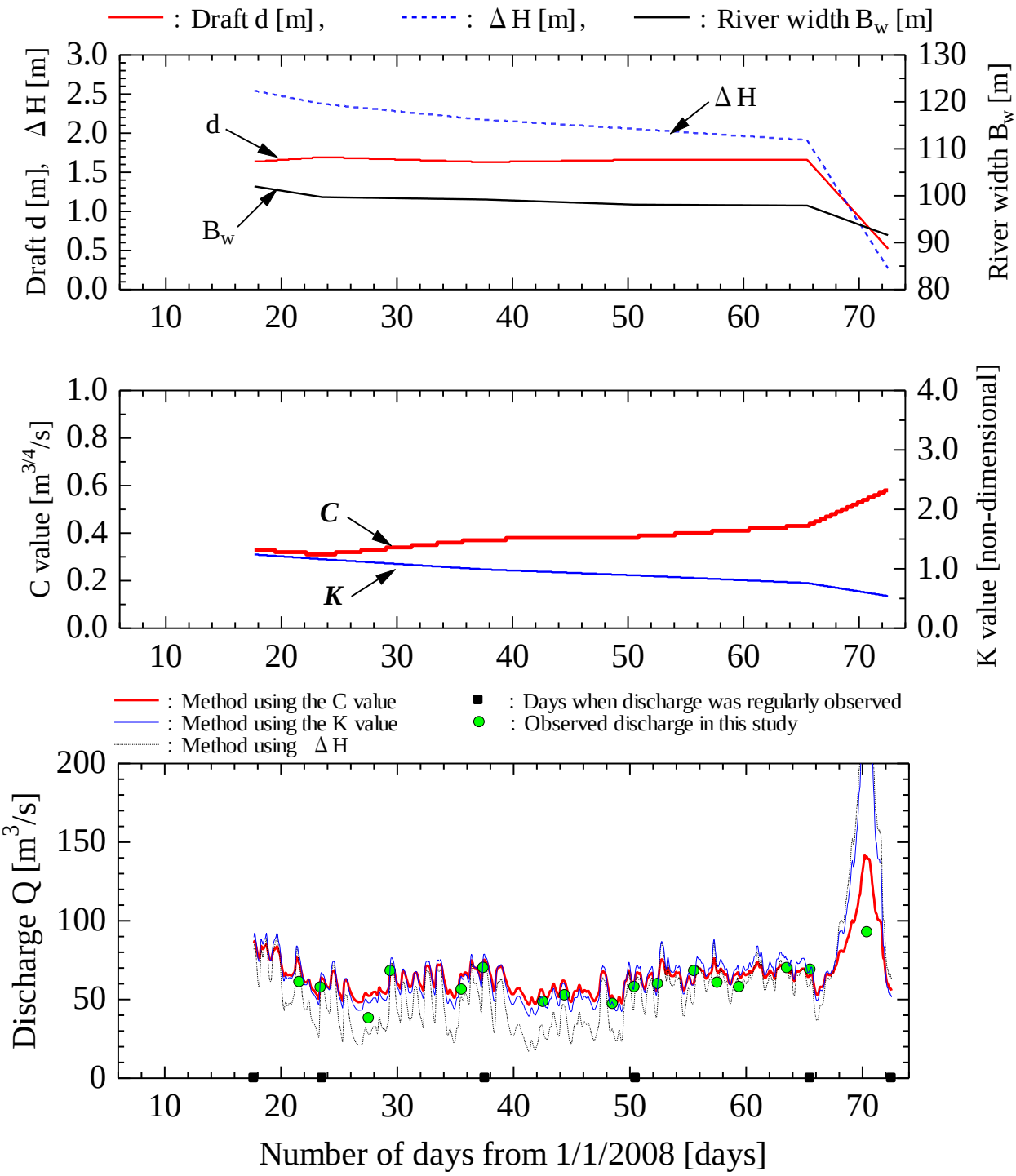

Figure 18 Estimated discharge using the new method vs. the conventional methods and observed discharge (Site C at KP 111.70)

Error histogram

Fig. 20 shows an error histogram of the estimated discharge in relation to the observed discharge. It was determined that the observed data used for error evaluation should be within the period of regular discharge observation of the frozen river, and 36 out of 40 observed discharge data sets obtained throughout this study were used.

According to Fig. 20, 12 data (33%, ΔH method), 13 data (36%, K method) and 13 data (36%, C method) of the total of 36 data sets were within a ±5% margin of error with the methods using ΔH, K and C, respectively, indicating a similar degree of accuracy for discharge estimation under each method. Similarly, 21 data (58%, ΔH method), 18 data (50%, K method) and 21 data (58%, C method) of the total of 36 data sets were within a ±10% margin of error with the methods using ΔH, K and C, respectively, while 29 data (81%, ΔH method), 29 data (81%, K method) and 33 data (92%, C method) of the 36 were within a ±20% margin of error with the methods using ΔH, K and C, respectively.

Data in which the error in flow rate estimated by the method using C exceeded 35% was obtained at the time when the volume of discharge from the Iwaonai Dam was 0 m^3/s and so the water level decreased dramatically. Here, C can be substituted and expressed by

$$C = \frac{\sqrt{I_e}}{n} R^{\frac{2}{3}} h_w^{-\frac{1}{4}} = \frac{\sqrt{I_e}}{n\, 2^{\frac{2}{3}}} h_w^{\frac{5}{12}} \tag{30}$$

In Eq. 30, the amount of change in C increases with a decrease in water depth h_w. It was thought that, in the period when C is linearly interpolated, flow rates cannot be estimated appropriately as the amount of change in C becomes greater when the water depth decreases dramatically.

With this level of accuracy, the new discharge estimation equation investigated in this study can be used to estimate discharge. In the study, the level of estimation accuracy of the new method was higher than that of the conventional methods. The accuracy of the equation is affected by continuous water level data, the estimation equation for the draft d Eq. 7 and the accuracy of the relationship between H' and A_o (Fig. 4). In the case where there is a change in the volume of river ice or its components, accumulation or traction of frazil or a change in water temperature during periods when d, C and B_w are given by a linear supplement, the estimated discharge is subject to these influences.

Advantages and disadvantages of the new method

It is difficult, for example, to identify the cause of a change in K because it is a coefficient of roughness for the open-water season and a function of the energy gradient, meaning that its value is affected by factors other than ice. However, the new method uses only observation data in the freezing season and includes a clear technique for estimating discharge. Accordingly, one advantage of this new approach is that it enables the causes of any inconsistency between estimated and observed discharge to be examined.

Disadvantages include the fact that it is not possible to estimate the influence of changes in the riverbed because the changes are not taken into consideration in the new method. Another drawback is the need to study how to determine snow density, ice sheet density and frazil density, which were given as constants in this study, in calculation of the draft d using Eq. 7; these values are expected to depend on place and time.

As this study has focused solely on the freezing period of rivers, further research is necessary to estimate discharge for the periods between the open-water season and the freezing season and between the freezing season and the melting season. Although the new method deals only with the freezing season of rivers, it was demonstrated that it increased accuracy in estimating discharge through the use of existing observation data without additional observations.

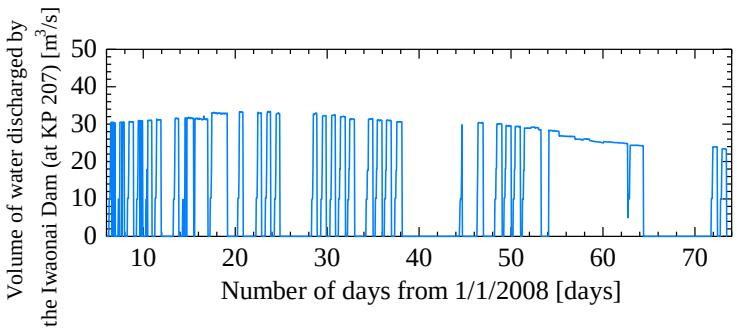

Figure 19 Temporal changes in the volume of water discharged by the Iwaonai Dam

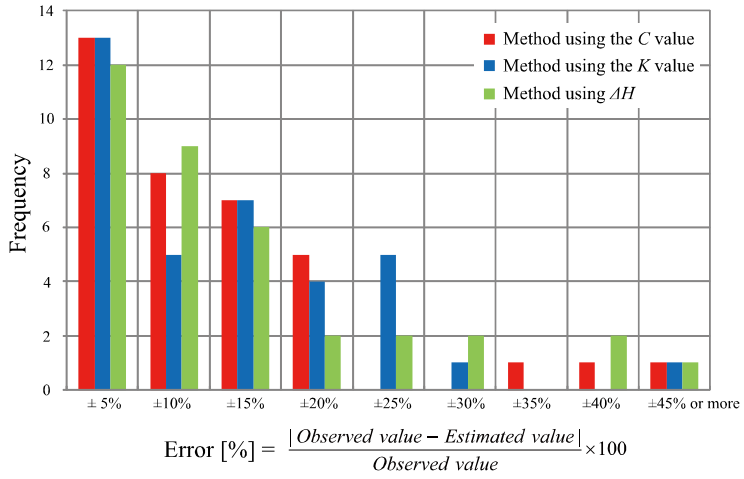

Figure 20 Error histogram of estimated discharge (total of 36 data sets)

CONCLUSION

The results of observations made this study reveal that the equivalent roughness k_s in the freezing season decreased over time. This was due to melting and smoothing of the river ice bottom by flowing water. Although the wall is thought to be rough based on the assumption that the flow path constitutes pipe flow in the freezing season, $k_s^{1/6}/(n\sqrt{g})$ cannot be handled as a constant in the Manning-Strickler equation. An equation to estimate the flow velocity coefficient ϕ in the freezing season using the hydraulic radius R and the energy gradient I_e was presented, and a new method of estimating discharge in the freezing season from C, the river width and the discharge area was developed. This approach does not depend on the H-Q curve of the open-water season, is applicable to sites with frazil accumulation, and allows estimation using only existing observation data. The accuracy of the estimated discharge within a ±20% margin of error was 92% for the total of 36 data sets. Findings of this study reveal that the estimation accuracy of the new method is higher than that of the conventional methods, and that discharge can be estimated on an ongoing basis from continually measured water levels by finding C, the draft d and the river width B_w through a linear supplement.

ACKNOWLEDGMENTS

The authors would like to express their gratitude to the Hokkaido Regional Development Bureau for the provision of data, as well as to Professor Hung Tao Shen of Clarkson University in the United States and Professor Shigeki Sakai of Iwate University for their valuable comments about this study.

REFERENCES

1. Kamata, S.: Ice formation and stream flow under conditions in rivers, Report of the Civil Engineering Research Institute, No. 38, pp. 10-16 and 51-56, 1965 (in Japanese).
2. Hung Tao Shen and Poojitha D. Yapa: Flow Resistance of River Ice Cover, Journal of Hydraulic Engineering, Vol. 112, No. 2, pp. 142-156, 1986.
3. Yoshikawa, Y., Watanabe, Y., Hayakawa, H., Seiji, M.: Continuous measurement of the thickness of frazil under ice, JSCE, Annual Journal of Hydraulic Engineering, Vol. 53, pp. 1027-1032, 2009 (in Japanese).
4. Yamashita, S.: A Study on River Discharge Estimation with Ice Cover, Monthly Report of the Civil Engineering Research Institute, No. 536, 1998 (in Japanese).
5. Hirayama, K.: Characteristics of Ice-covered Streams in Connection with Water Discharge Measurements, IAHR Ice Symposium, Vol. 2, Lulea, Sweden, 1978.
6. Hirayama, K.: Characteristics of Ice-covered Streams in Connection with Water Discharge Measurements (Part II), Hokkaido Advisory Committee on Water Use, Review of Water Use, Vol. 27, pp. 27-55, 1983 (in Japanese).
7. Abashiri Development Construction Department, Hokkaido Development Bureau: Survey and Analysis of Water Discharge Measurements in Winter, pp. 62-77, 1979 (in Japanese).
8. Yoshikawa, Y., Watanabe, Y., Hayakawa, H., Hirai, Y.: Development of a Practical Equation for Calculating the Thickness of Ice Sheets, JSCE, Proceedings of the 64th Annual Conference of the Japan Society of Civil Engineers, pp. 127-128, 2009 (in Japanese).
9. Moody, F. F.: Friction Factors for Pipe Flow, Trans. ASME, Vol. 66, p. 671, 1944.
10. Tsubaki, T.: Hydraulics I, Morikita Publishing, pp. 99 and 109, 1988 (in Japanese).
11. George D. Ashton, Ed.: River Lake Ice Engineering, Water Resources Publications, pp. 233-236 and 289, 1986.

APPENDIX – NOTATION

The following symbols are used in this paper:

Q = discharge [m^3/s];

A_o = discharge area [m^2];

A_i = ice sheet area [m^2];

A_f = frazil area [m^2];

n = Manning's coefficient of roughness [$s/m^{1/3}$];

R = hydraulic radius [m];

I_e = energy gradient [non-dimensional];

α = energy coefficient [non-dimensional];

u_m = sectional average flow velocity [m/s];

g = gravity acceleration [m/s^2];

H = water level [m];

ϕ = flow velocity coefficient [non-dimensional];

u_* = friction velocity [m/s];

B_w = river width [m];

d = draft [m];

ρ = density [kg/m^3];

S = wetted perimeter [m];

h_w = effective depth [m];

Z = average bed height [m];

f = friction factor [non-dimensional];

D = pipe diameter [m];

k_s = equivalent roughness [m];

h_{id} = river ice thickness near flowing water affecting the bottom shape [m];

L_i = latent heat of ice [J/kg];

ϕ_w = heat flux from the flowing water to the river ice bottom [W/m^2];

C_{wi} = coefficient [W・S$^{0.8}$・°C^{-1}・m$^{-2.6}$];

T_w = water temperature [°C];

T_{id} = temperature at the river ice bottom [°C];

C_o = coefficient [m$^{1/4}$]; and

C = coefficient [m$^{3/4}$/s], indicates the degree of decrease in roughness caused by melting and smoothing of the river ice bottom by flowing water.